Numerical and experimental analysis of carotid artery blood flow

NUMERICAL AND EXPERIMENTAL ANALYSIS OF CAROTID ARTERY BLOOD FLOW

A.A. van Steenhoven, C.C.M. Rindt, R.S. Reneman[+] and J.D. Janssen

Department of Mechanical Engineering, Eindhoven University of Technology, Eindhoven, The Netherlands

Department of Physiology, University of Limburg Maastricht, The Netherlands

ABSTRACT

To obtain more insight into the complex blood flow patterns in the carotid artery bifurcation, finite element calculations have been carried out combined with flow visualization studies and laser-Doppler velocity measurements. As curvature effects are expected to be important in a bifurcation, first the steady flow development in a curved tube was investigated. From a detailed analysis of steady flow in a three-dimensional model of the carotid artery bifurcation it is concluded that curvature effects indeed play an important role in the daughter branches of this bifurcation, but also that the local geometry of the carotid sinus highly affects the axial and secondary flow fields. In general a good agreement is found between the numerical and experimental results.

KEYWORDS

Bend, carotid artery bifurcation, finite element analysis, visualization studies, laser-Doppler measurements.

INTRODUCTION

In the development of non-invasive detection methods of atherosclerotic lesions in the carotid artery bifurcation at an early stage of the disease, insight into the complicated flow field in this bifurcation is indispensable. The geometry of this bifurcation is shown in figure 1. It consists of a main branch, the common carotid artery, which asymmetrically divides into two branches, the internal and external carotid arteries. The internal carotid artery is characterized by a widening in its most proximal part, the sinus or bulb. Detailed experimental information about the flow field in this bifurcation has been obtained for the steady case by Bharadvaj et al.(1982) and for the unsteady case by Ku et al.(1983).

The aim of the present study is to develop an accurate numerical model of fluid flow in the carotid artery bifurcation. With such a model the influences of interindividual variabilities in geometry and the presence of small stenoses on the flow field can be quantified. The geometry used in this study is similar to that used by Bharadvaj et al.(1982); the characteristic dimensions are shown in figure 1. Both calculations and measurements were carried out enabling an experimental validation of the numerical model. In earlier studies, the numerical (Cuvelier et al.,1986 and van de Vosse et

Biomechanical Transport Processes, Edited by F. Mosora *et al.*
Plenum Press, New York, 1990

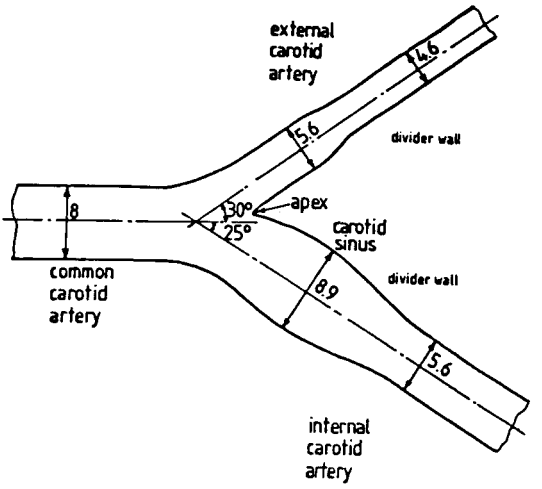

Figure 1. Schematical presentation of the human carotid artery bifurcation (Adapted from Bharadvaj et al., 1982).

al.,1986) and experimental methods (Corver et al.,1985 and van Steenhoven et al.,1988) were described. Besides, in an experimental and numerical study by van de Vosse et al.(1985) steady and pulsatile flow over a two-dimensional square step was analysed. Rindt et al.(1987) performed steady and unsteady velocity measurements and calculations of fluid flow in a two-dimensional model of the carotid artery bifurcation. A study by van de Vosse et al.(1990) indicated that three-dimensional analysis of the flow field in the carotid artery bifurcation is necessary to better understand the in vivo flow situation. To gain more insight into the secondary flow patterns and because of its geometrical simplicity, first steady entrance flow in a 90-degree bend was studied. Bovendeerd et al.(1987) performed laser-Doppler velocity measurements in such a bend, while three-dimensional calculations were reported by van de Vosse et al.(1989) and Rindt (1989). Next, the steady flow in a three-dimensional model of the carotid artery bifurcation was analysed, using experimental (Rindt et al.,1989) and numerical (Rindt et al.,1990) techniques. In all those studies a reasonable agreement was found between the numerical and experimental results.

In this paper the numerical and experimental methods used will be briefly described and some characteristic results for steady flow in a 90-degree bend and in a 3D-model of the carotid artery bifurcation will be presented. For the sake of clearness the total flow field will be divided into axial and secondary flow fields, the latter defined as the flow field in a cross-section perpendicular to the tube axis. The results will be shown at a Reynolds number, based on the diameter of the common carotid artery, of about 700. The flow division ratio between the internal and external carotid arteries is chosen to be about 50/50. Both numbers correspond to the peak systolic values of blood flow in the carotid artery bifurcation (Ku et al.,1983)

NUMERICAL METHOD

Flow of an incompressible and isothermal fluid is described by the momentum and continuity equations. Neglecting gravity effects, for steady flow these equations read in dimensionless form:

$$\vec{u}\cdot\vec{\nabla}\vec{u} - \vec{\nabla}\cdot\sigma = \vec{0} \quad ; \quad \vec{\nabla}\cdot\vec{u} = 0 \qquad (1)$$

with $\vec{u}$ the velocity vector, σ the Cauchy stress tensor and $\vec{\nabla}$ the gradient vector operator. In this study only Newtonian fluids will be considered for which the Cauchy stress tensor is coupled to the velocity field as:

$$\sigma = - pI + \frac{1}{Re} [\vec{\nabla}\vec{u} + (\vec{\nabla}\vec{u})^C] \quad ; \quad Re = \frac{DU}{\nu} \tag{2}$$

with p the pressure, I the unit tensor and $(\vec{\nabla}\vec{u})^C$ the conjugate of the velocity gradient tensor. Re denotes the Reynolds number and its value is calculated from the diameter (D) and mean velocity (U) at the inlet and the kinematic viscocity ν of the fluid.

The numerical method used is based on a Galerkin finite element approximation of equations 1 and 2, which leads to the following set of non-linear equations (Cuvelier et al.,1986):

$$[N(\underline{U}) + S]\underline{U} + L^T\underline{P} = \underline{B} \quad ; \quad L\underline{U} = \underline{0} \tag{3}$$

Here $N(\underline{U})\underline{U}$ represents the convective acceleration term, $S\underline{U}$ the viscous term, $L^T\underline{P}$ the pressure gradient term and $L\underline{U}$ the velocity divergence term. $\underline{B}$ represents the boundary forces and $\underline{U}$ contains the velocity and $\underline{P}$ the pressure unknowns in the nodal points. To avoid partial pivoting this set of equations is uncoupled with the penalty function method. The non-linear convective term $N(\underline{U})\underline{U}$ is linearised by a Newton-Raphson iteration method. The construction of the system of equations, its solution and the post-processing of the velocity data is carried out with the finite element package SEPRAN (Segal,1984).

The discrete points, in which velocities and pressures are calculated, are determined by partition of the 3D-geometry into elements. The 3D element used is the so-called Crouzeix-Raviart element, shown in figure 2a. It has 27 nodes for the velocity (triquadratic, 81 velocity unknowns) and 1 node for

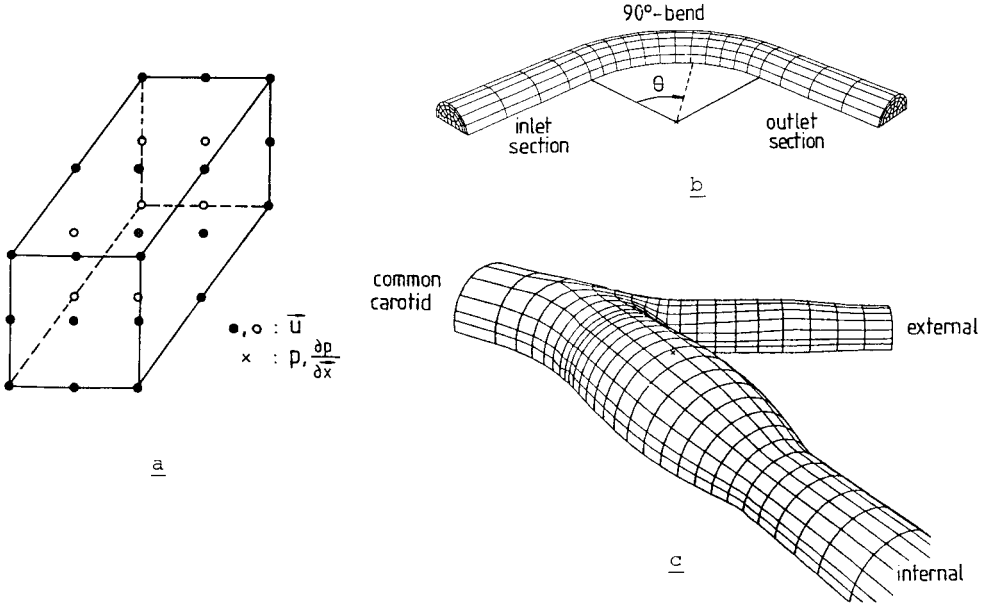

Figure 2. The element used (a) and the element divisions for the 90-degree curved tube (b) and the carotid artery bifurcation (c).

the pressure (linear, 4 pressure unknowns). Due to the triquadratic approximation within the element the velocity has a third order accuracy. Figure 2b shows the element division used for the analysis of the steady entrance flow in a bend. It consists of 20 elements in axial direction and 30 elements per cross-section. Figure 2c shows a plot of the element division of the carotid artery bifurcation, where 1474 elements were used.

For both geometries similar boundary conditions were used. Flow at the inlet was supposed to be fully developed, which means a parabolic axial velocity profile and zero secondary velocities. The velocities at the wall were presumed to be zero, according to the no-slip condition. At the outlet the normal and both tangential stresses were set to zero, while in the plane of symmetry both tangential stresses and the normal velocity component were put to zero.

EXPERIMENTS

In figure 3a the experimental set-up is shown for the visualization experiments and velocity measurements under steady flow conditions. By means of a voltage controlled gear pump P the fluid was pumped from the reservoir R into the measurement section. A long circular pipe upstream of the model was used to ensure a fully developed pipe flow at its entrance. The 3D-models consisted of two halves of perspex, split at the plane of symmetry, in which the 90-degree curved tube and the carotid artery bifurcation were machined out. In figure 3b the models used for the laser-Doppler experiments are presented; for the visualization experiments 5 times enlarged models were used. The ratio of tube radius and curvature radius for the bend was chosen to be 1/6, resembling more or less the geometry of the entrance region of the internal carotid artery.

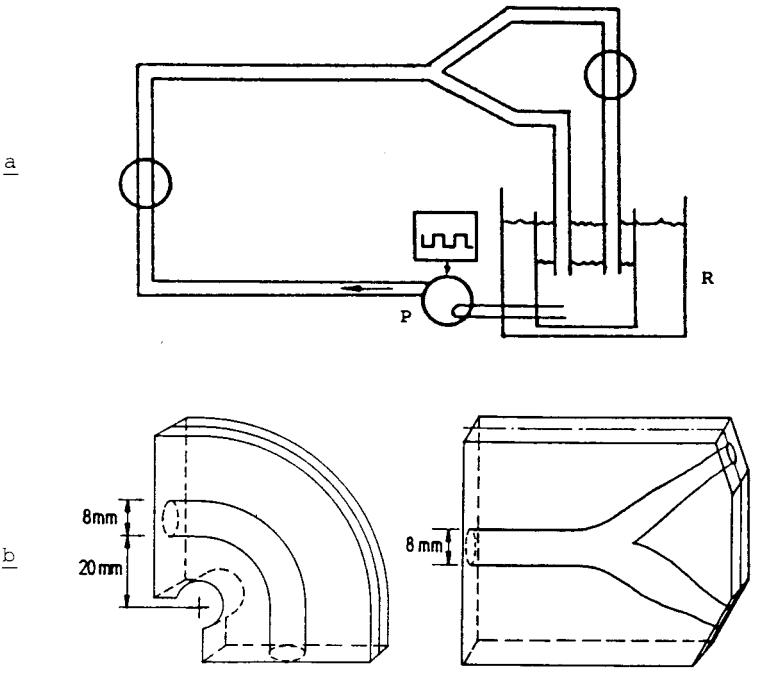

Figure 3. Fluid circuit as used in the experiments (a) together with the perspex models of the 90-degree curved tube and the carotid artery bifurcation (b).

The fluid flow was visualized with the use of the hydrogen bubble technique, as described by Merzkirch (1974). The cathode is a thin (20 μm) platinum wire positioned in the flow field to be studied. The anode is a stainless-steel plate located in such a place that is does not disturb the flow. The fluid used was demineralized water to which a small amount of an electrolyte (0.5% acetic acid) was added. Hydrogen bubbles are produced periodically at the cathode by a square wave generator. The axial flow field in the symmetry plane of the 90-degree curved tube was visualized simultaneously at two locations (0 and 38 degrees) along the bend. To visualize the secondary flow patterns also sheets of hydrogen bubbles were produced applying a dc voltage between the electrodes. In that case the cathode wire was placed out of the plane of symmetry.

The fluid velocity was measured by a one-component laser-Doppler instrument (DISA, measuring volume = 400 μm x 40 μm x 40 μm), based on the forward-scattering reference-beam method. A Bragg cell was used to discriminate velocity directions. Velocity measurements in 3D-geometries require exact matching of the refraction indices of the fluid and of the perspex models. Therefore, as circulating fluid a mixture of oil (Shellflex 214 BG) and kerosine was used. The experiments were performed at 40^0C to lower the kinematic viscosity of the oil mixture and to eliminate the influence of ambient temperature variations. For seeding silicagel (Lichrosorb, Si 100, mean particle diameter 5 μm) was used. Three stepper motors were used to traverse the model in three independent directions, through which positioning of the measuring volume at various sites in the model was possible with an accuracy of about 5 μm in each direction. Independently, the axial velocity component and both secondary velocity components were measured in about 100 grid points per cross-section. For each measurement 10 samples were taken from which the mean value and the 95% confidence interval were calculated. A personal computer was used to control the traversing mechanism and the data acquisition.

RESULTS

In figure 4 the results of the flow visualization in the 90-degree bend are shown. In the upper panel the axial flow field is visualized in the plane of symmetry. Due to the centrifugal forces the profiles remain not axial symmetric. The maximum velocities occur near the outside wall, while at the inner wall a so-called velocity plateau is formed. Due to the interaction of centrifugal, pressure, and viscous forces two helical vortices develop; one at each side of the plane of symmetry. This pattern is visualized for the upper half in the lower panel of figure 4.

In figure 5a the axial velocity profiles in the plane of symmetry are presented for both the laser-Doppler measurements and the finite element calculations. A similar shift to the outer bend is found as observed from the visualization experiments. There is a fair agreement between the experimental and numerical data, although in the numerical case the axial velocity plateau at 58.5 degrees is somewhat less developed. In figure 5b the calculated and measured secondary flow fields at 23.4 and 58.5 degrees are presented by velocity profiles of the component parallel to the plane of symmetry (upper half) and the component perpendicular to the plane of symmetry (lower half). As shown in this figure and visualized in figure 4, the secondary velocities near the plane of symmetry are directed from the inner bend towards the outer bend, while near the side wall a circumferentially inward motion of the fluid occurs. Here again a good agreement exists between the experimental and numerical results.

In figure 6 the visualized flow field in a 3D-model of the carotid artery bifurcation is shown. The visualization wires are placed perpendicular to the plane of symmetry. From this figure it is concluded that also at the entrance of the internal carotid artery secondary motions are present.

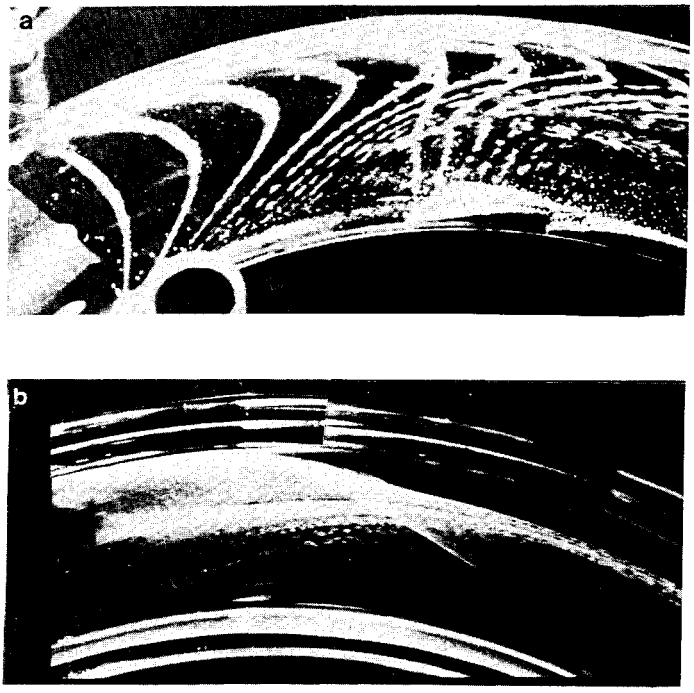

Figure 4. Flow visualization in the plane of symmetry (a) and in the upper half (b) of the 90-degree curved tube (Re = 840).

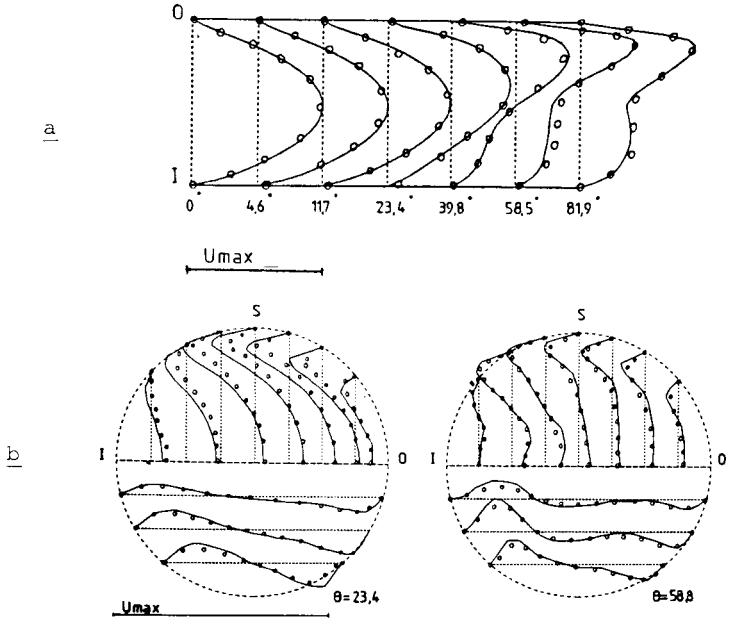

Figure 5. Calculated (-) and measured (ooo) axial velocity profiles in the plane of symmetry (a) and secondary velocity profiles at two cross-sections (b) of the 90-degree curved tube (Re = 640, I: inner wall, 0: outer wall, S: side wall).

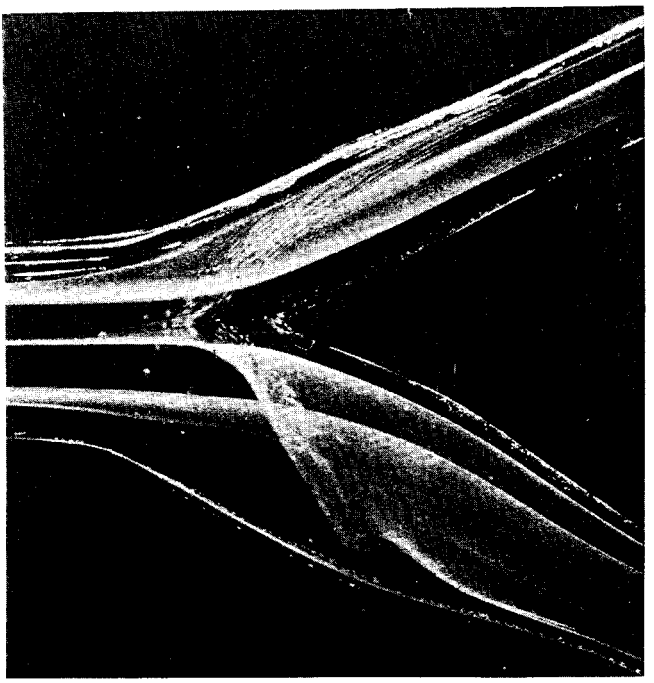

Figure 6. Flow visualization in a 3D-model of the carotid artery bifurcation (Re = 900).

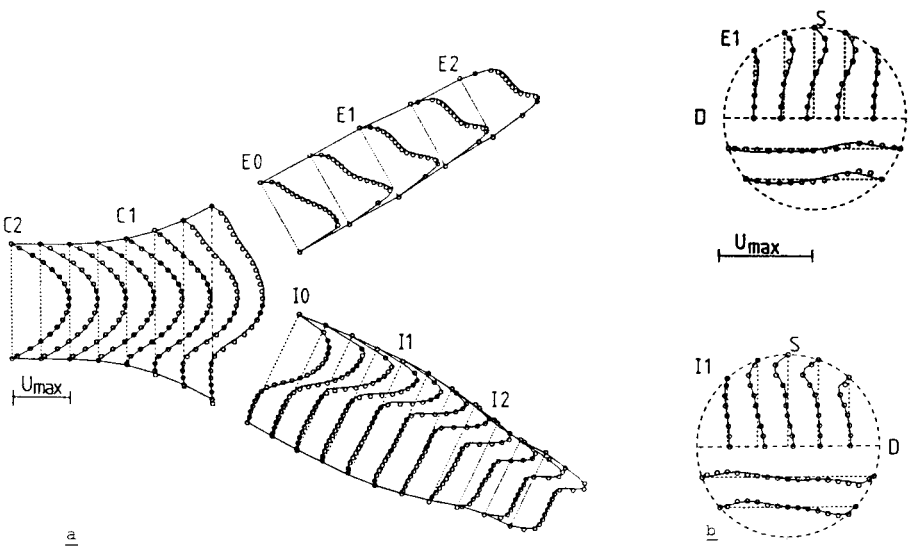

Figure 7. Calculated (-) and measured (ooo) axial velocity profiles in the plane of symmetry (a) and secondary velocity profiles at two cross-sections (b) of the carotid artery bifurcation (Re = 640, D: divider wall, S: side wall). From Rindt et al.(1990), with permission.

In figure 7a the axial velocity profiles in the plane of symmetry of the bifurcation are presented for both the laser-Doppler measurements and the finite element calculations. The characters C, I and E refer to the common, internal and external carotid arteries and the numbers to axial distances to the flow divider expressed in diameters of the main branch. In the model common carotid artery (C1.5) the velocity profile is parabolic. At the entrance of the internal carotid artery high axial velocities are found near the divider wall, which is primarily caused by flow branching. A region with negative axial velocities with a diameter up to 60% of the local diameter of the bulb is found opposite to the flow divider. The agreement between the experimental and numerical data is good. In figure 7b the profiles of the secondary velocity components are shown at positions one diameter downstream in the internal and external carotid arteries. Near the plane of symmetry the secondary velocities are directed towards the divider wall and near the side wall they point circumferentially back towards the non-divider wall. There is again a fair agreement between the numerical and experimental data.

CONCLUDING DISCUSSION

From the present study it is concluded that the finite element method can be used for detailed analyses of fluid flow in complex three-dimensional geometries. The findings in this study also indicate that qualitatively the secondary flow fields in a curved pipe and halfway the carotid sinus show remarkable similarities, although other results (Rindt et al.,1990) suggest that at the entrance and end of the bulb the secondary flow fields are also highly influenced by the specific geometry of the carotid sinus. Both findings support the statement of Olsen (1971) that the flow phenomena in a symmetrical bifurcation with straight daughter branches mainly originate from curvature effects. On the contrary to the flow in a 90-degree curved tube, a large region with reversed axial flow is observed opposite to the flow divider in the internal carotid artery. These negative axial velocities are mainly due to the divergent geometry of the inlet section of the carotid sinus. The width of the region is somewhat larger than the value reported by Bharadvaj et al.(1982), probably due to the higher flow division ratio (70/30) used by them.

In the near future the unsteady flow phenomena in the carotid bifurcation will be investigated. Next, the influence of the wall flexibility on the axial and secondary flow fields has to be evaluated. To that end, the analysis of wave propagation of pressure and flow pulses (van Steenhoven and van Dongen,1986 and Horsten et al.,1989) has to be incorporated in the numerical model. A strategy and some preliminary results have been described by Reuderink et al.(1989).

ACKNOWLEDGEMENTS

We thank W. Vegt and F. Smeets for performing the visualization experiments and J.W.G. Cauwenberg and L.H.G. Wouters for their technical assistance.

REFERENCES

Bharadvaj B.K., Mabon R.F. and Giddens D.P. (1982). Steady flow in a model of the human carotid bifurcation, Part 1- Flow visualization, Part 2- Laser-Doppler anemometer measurements, J. Biomechanics, 15: 349-378.

Bovendeerd P.H.M., van Steenhoven A.A., van de Vosse F.N. and Vossers G.(1987). Steady entry flow in a curved pipe, J. Fluid Mech., 177: 233-246.

Corver J.A.W.M., van de Vosse F.N., van Steenhoven A.A. and Reneman R.S. (1985).The influence of a small stenosis in the carotid bulb on adjacent velocity profiles, in: "Biomechanics Current Interdisciplinary Research", S.M. Perren and E. Schneider eds., 239-244, Martinus Nijhoff Publ., Dordrecht.

Cuvelier C., Segal A. and van Steenhoven A.A. (1986). "Finite Element Methods and Navier-Stokes Equations", D. Reidel Publ., Dordrecht.

Horsten J.B.A.M., van Steenhoven A.A. and van Dongen M.E.H. (1989). Linear propagation of pulsatile waves in viscoelastic tubes, J.Biomechanics, 22: 477-484.

Ku D.N. and Giddens D.P. (1983). Pulsatile flow in a model carotid bifurcation, Arteriosclerosis, 3: 31-39.

Merzkirch W. (1974). "Flow Visualization", Academic Press, New York.

Olson D.E. (1971). Fluid mechanics relevant to respiration: flow within curved or elliptical tubes and bifurcating systems, Ph.D-thesis, University of London.

Reuderink P.J., Willems P.J.B., Schreurs P.J.G. and van Steenhoven A.A.(1989). Fluid flow through distensible models of the carotid artery bifurcation, Proceedings Second International Symposium on Biofluid Mechanics, 455-461, München.

Rindt C.C.M, van de Vosse F.N., van Steenhoven A.A., Janssen J.D. and Reneman R.S.(1987). A numerical and experimental analysis of the flow field in a two-dimensional model of the human carotid artery bifurcation, J.Biomechanics, 20: 499-509.

Rindt C.C.M., van Steenhoven A.A. and Reneman R.S.(1988). An experimental analysis of the flow field in a three-dimensional model of the human carotid artery bifurcation, J.Biomechanics, 21: 985-991.

Rindt C.C.M., van Steenhoven A.A., Janssen J.D., Reneman R.S. and Segal A.(1990). A numerical analysis of steady flow in a 3D-model of the carotid artery bifurcation, J.Biomechanics, in press.

Segal A.(1984). "Sepran User Manual and Programmers Guide", Ingenieursburo Sepra, Leidschendam.

Van de Vosse F.N., Vial F.H., van Steenhoven A.A., Segal A. and Janssen J.D.(1985). A finite element and experimental analysis of steady and pulsating flow over a two-dimensional step, in: "Numerical Methods in Laminar and Turbulent Flow", C. Taylor ed., 515-526, Pineridge Press, Swansea.

Van de Vosse F.N., Segal A., van Steenhoven A.A. and Janssen J.D.(1986). A finite element approximation of the unsteady 2D'Navier-Stokes equations, Int.J.Num.Meth.Fluids, 6: 427-443.

Van de Vosse F.N., van Steenhoven A.A., Segal A. and Janssen J.D.(1989). A finite element analysis of the steady laminar entrance flow in a 90^0 curved tube, Int.J.Num.Meth.Fluids, 9: 275-287.

Van de Vosse F.N., van Steenhoven A.A., Janssen J.D. and Reneman R.S.(1990). A two-dimensional numerical analysis of unsteady flow in the carotid artery bifurcation, Biorheology, accepted.

Van Steenhoven A.A. and van Dongen M.E.H.(1986). Model studies of the aortic pressure rise just after valve closure, J. Fluid Mech., 66: 93-113.

Van Steenhoven A.A., van de Vosse F.N., Rindt C.C.M., Janssen J.D. and Reneman R.S.(1990). Experimental and numerical analysis of carotid artery blood flow, in: "Blood flow in large arteries: Applications to atherogenesis and clinical medicine", D.W. Liepsch ed., 250-260, Monogr. Atheroscler. vol. 15, Karger, Basel.